

Large-Scale Synthesis and CO Oxidation Study of FeCr Alloy Supported Pt Nanocatalyst by Electrical Wire Explosion Process

Jung Yeul Yun · A. Satyanarayana Reddy · Sangsun Yang ·
Hyeon Ju Kim · Hye Young Koo · Hye Moon Lee ·
Chan Ho Jung · Kamran Qadir · Sunmi Kim ·
Jeong Young Park

Received: 10 August 2011 / Accepted: 6 January 2012 / Published online: 31 January 2012
© Springer Science+Business Media, LLC 2012

Abstract Platinum nanoparticles supported on FeCr alloy have been synthesized at a large-scale by sequential electrical explosion of FeCr alloy and Pt wires in ethanol. X-ray diffraction showed corresponding peaks of non-oxide phase Pt and FeCr alloy nanoparticles. Transmission electron microscopy showed uniform dispersion of Pt nanoparticles on the support with an average size of 2 nm and high thermal stability up to 600 °C. These Pt-FeCr alloy nanoparticles were found to be active for CO oxidation with an activation energy of 15 kcal mol⁻¹ and negligible deactivation. This work demonstrated the application of the electrical wire explosion process for synthesis of supported metal catalysts with high thermal stability and activity.

Keywords Electrical wire explosion · Pt-Fe nanoparticles · Nanocatalyst · CO oxidation

1 Introduction

Recently, the demand for rapid large-scale synthesis of nanomaterials by effective and low-cost methods has increased due to potential applications in nanotechnology and catalysis [1, 2]. To obtain higher catalytic activity, a high dispersion of metal nanoparticles on the support

material is desired, where metal oxides are commonly used as support materials. The use of metal/alloys provides high thermal stability due to the strong chemical bonds that form between the alloy and the active metal on the surface [3–7]. The use of metal nanoparticles in high temperature catalytic reactions has prompted great attention to be paid to the synthesis of thermally stable nanocatalysts [8, 9]. The overall performance of a supported metal nanocatalyst depends highly on the size and shape of the nanoparticles, the structure and properties of the oxide supports, and metal-oxide interactions [4, 10]. Most common techniques used to prepare oxide-supported nanoparticles include co-precipitation and deposition precipitation [11, 12]. All of the conventional synthesis methods use an organic capping agent to control the size and shape of the active metal or support nanoparticles. Nanoparticles with capping layers are not suitable for high temperature (>300 °C) reactions, such as CO oxidation [8], partial oxidation [13], hydrocarbon cracking [14], combustion [15], and ignition behavior studies [16], as the capping molecules decompose and cause aggregation of the nanoparticles. Furthermore, these methods are time consuming, not suitable for large-scale synthesis, nor applicable for all metals and metal oxides. Hence, the faster, large-scale synthesis methods known in powder technologies, such as gas-phase chemical reaction [17], spray pyrolysis [18], laser ablation [19], flame processing [20], and vapor deposition [21], can be used to synthesize catalytic nanomaterials. These methods are widely used in the catalyst community, however, owing to the difficulty in controlling synthesis parameters that are crucial for optimal catalytic performance. Considering the demand for rapid and large scale synthesis of supported metal catalysts, the electrical wire explosion (EWE) process appears to be a promising method to produce nanomaterials with new properties [22]. Non-oxide

J. Y. Yun (✉) · S. Yang · H. J. Kim · H. Y. Koo · H. M. Lee
Functional Materials Division, Korea Institute of Materials
Science (KIMS), Chang-won 641-831, South Korea
e-mail: yjy1706@kims.re.kr

A. S. Reddy · C. H. Jung · K. Qadir · S. Kim · J. Y. Park (✉)
Graduate School of EEWS (WCU), and NanoCentury KI,
KAIST, Daejeon 305-701, South Korea
e-mail: jeongypark@kaist.ac.kr

phase nanoparticles can be produced when the EWE method is conducted in liquid media. In this process, a thin metal or alloy wire in certain gas and/or liquid media is exploded using a large impulse current. This method is particularly advantageous because of the high yield and short reaction time [23].

In this study, we aimed to synthesize high-temperature stable alloy nanoparticles using the electrical wire explosion method to explore alternative synthesis methods for nanocatalysts. The Pt-FeCr alloy nanoparticles produced by the EWE process exhibit high thermal stability ($>600\text{ }^{\circ}\text{C}$) and are suitable for high temperature reactions. High thermal stability is important to retain the initial structure of the nanoparticles both during pretreatment and the course of the reaction by overcoming sintering effects. CO oxidation, a model reaction, has been investigated using these alloy nanoparticles to explore the catalytic performance of nanoparticles synthesized by the EWE process. The alloy nanoparticles were characterized by x-ray diffraction, transmission electron microscopy and x-ray photoemission spectroscopy.

2 Materials and Methods

2.1 Synthesis of Pt-FeCr Alloy Nanoparticles

Pt-FeCr alloy nanoparticles were synthesized by the EWE method (Fig. 1) in ethanol using Pt and FeCr alloy wires as source materials [22]. In this method, a metal wire was installed between high-voltage electrodes, which were connected to a $60\text{ }\mu\text{F}$ capacitor bank through a triggered spark gap switch. The wires were continuously fed by a feeding roller installed on the exploding vessel and were guided by a nozzle into the vessel. A voltage of 2.0 kV was applied to the metal wire. The metal wire overheated and evaporated swiftly when a very strong pulse current (current density of $2.9 \times 10^8\text{ A cm}^{-2}$) passed through the wire, resulting in an explosion. The expansion duration could be as short as several tens of microseconds [24]. FeCr alloy wires were exploded and subsequently condensed in ethanol. Then, Pt wires with a diameter of 0.1 mm were exploded and subsequently condensed in the FeCr alloy colloidal solution. Preparation of nanoparticles in ethanol by the electrical wire explosion process has several advantages over conventional wire explosion in air. By this process, a non-oxide metal powder can be formed without requiring vacuum conditions. These non-oxide phases remain dispersed in ethanol and are stable for several days. Further investigation is required to determine why these alloy nanoparticles do not aggregate. One possible explanation would be the contribution of an electrostatic force due to surface charges on the nanoparticles that

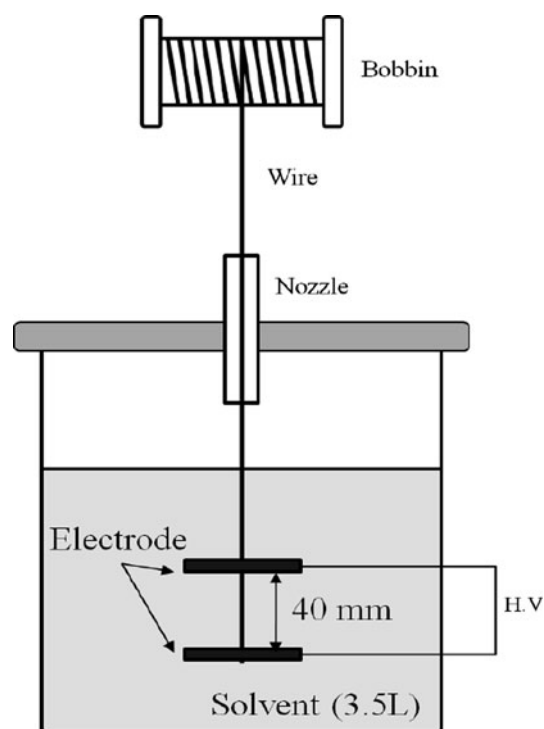


Fig. 1 Schematic of the electrical wire explosion process for the synthesis of Pt-FeCr alloy nanoparticles

keep them apart. These nanoparticles can be harvested by evaporating the ethanol to form the powder sample which can be used in conventional fixed bed flow reactors.

The sequential explosion of FeCr alloy and Pt wires formed highly dispersed FeCr alloy and Pt nanoparticles, respectively. The particle size of the alloy nanoparticles can be controlled by using different wire diameters. The $15.4 \pm 1.5\text{ nm}$ FeCr alloy nanoparticles were produced using a 0.2 mm wire [22]. Platinum wires were exploded and subsequently condensed in the FeCr alloy colloidal solution to produce highly dispersed Pt on the FeCr alloy nanoparticles. In the EWE process, the wire is usually overheated and evaporated swiftly when a very strong pulse current with high current density passes through it, resulting in explosions that produce a shock wave, yielding metal powders. Unless complete evaporation of the metal wire occurs due to an excess supply of energy in the EWE process, the wire splits into metal vapors and overheated metal droplets [25]. The overheated metal droplets formed by incomplete evaporation of the wire form submicro- and micrometer sized particles.

2.2 Characterization

The Pt-FeCr alloy nanoparticles synthesized by the EWE method were analyzed using powder x-ray diffraction to

determine the crystal structure on a D-Max 2200 (RIGAKU, JPN). The morphology, size, and composition of the Pt-FeCr nanoparticles were investigated by transmission electron microscopy and energy dispersive spectroscopy using a JEM-2100F (JEOL, JPN). The surface composition and constituents of the alloy nanoparticles were analyzed by x-ray photoelectron spectroscopy using a Sigma Probe (Thermo VG Scientific) instrument equipped with an Al-K α x-ray source (1486.3 eV).

2.3 Catalytic Activity

CO oxidation was performed in an ultrahigh-vacuum batch reactor (1L) with a base pressure of 5.0×10^{-8} torr [26]. A thin film of Pt-FeCr alloy nanoparticles deposited on a Si wafer ($0.7 \times 1.1 \text{ cm}^2$), using the drop casting method, was mounted in the reaction chamber. The reaction chamber was evacuated and isolated with a gate valve before it was charged with 40 torr CO, 100 torr O₂ and 620 torr He at room temperature. The reaction mixture was circulated continuously through the reaction line by a metal-bellows recirculation pump at a rate of 2 L min^{-1} . The CO conversion was monitored as a function of reaction temperature (180–230 °C). The reaction mixture was continuously analyzed through an online GC. A DS 6200 gas chromatograph equipped with a thermal conductivity detector and a 15' long, 18' outer diameter stainless steel 60/80 mesh size carboxen-1000 (Supelco) column was used to separate the reaction mixture for analysis. Percentage CO conversion was reported and calculated based on the CO₂ product molecules produced per weight of the catalyst per second of reaction time.

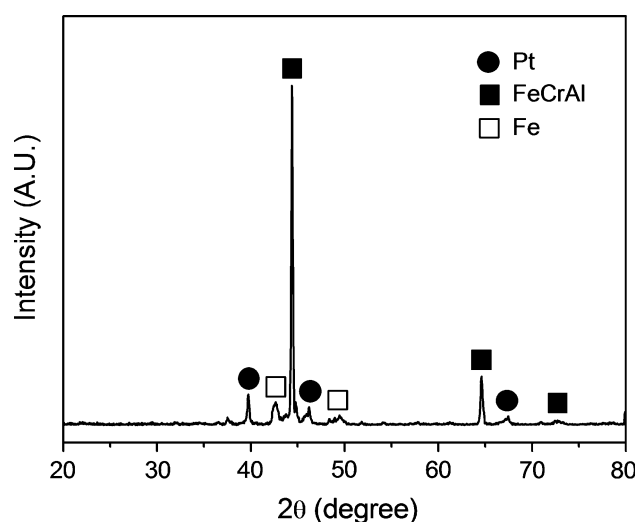


Fig. 2 X-ray diffraction patterns of Pt-FeCr alloy nanoparticles formed by the electrical wire explosion process after calcination at 600 °C

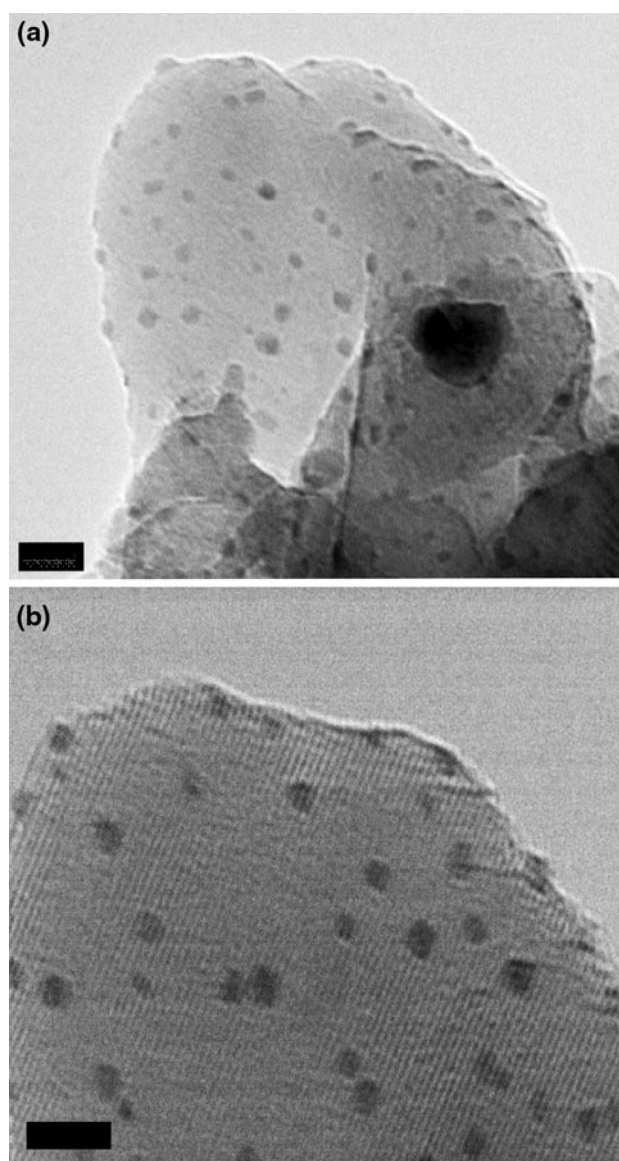


Fig. 3 Transmission electron microscopy images of Pt-FeCr alloy nanoparticles produced by the electrical wire explosion process after being calcined at 600 °C. Scale bar equivalent to 5 nm

3 Results and Discussion

As the synthesis process of the Pt-FeCr alloy nanoparticles involved sequential production of the support FeCr alloy and Pt nanoparticles, a majority of the Pt nanoparticles (2 nm) were found deposited on the support, as studied by spot-energy dispersive spectroscopy (EDS) analysis. However, the presence of free Pt nanoparticles cannot be ruled out, but they make up less than 5% of the total Pt nanoparticles studied by EDS analysis. The geometric size distributions of the FeCr alloy and Pt nanoparticles were reported earlier [22] and the average size of the FeCr alloy and Pt nanoparticles were found to be 15.4 and 2 nm,

Fig. 4 X-ray photoemission spectra of Pt-FeCr alloy nanoparticles **a** Pt4f, **b** Fe2p, and **c** Cr2p

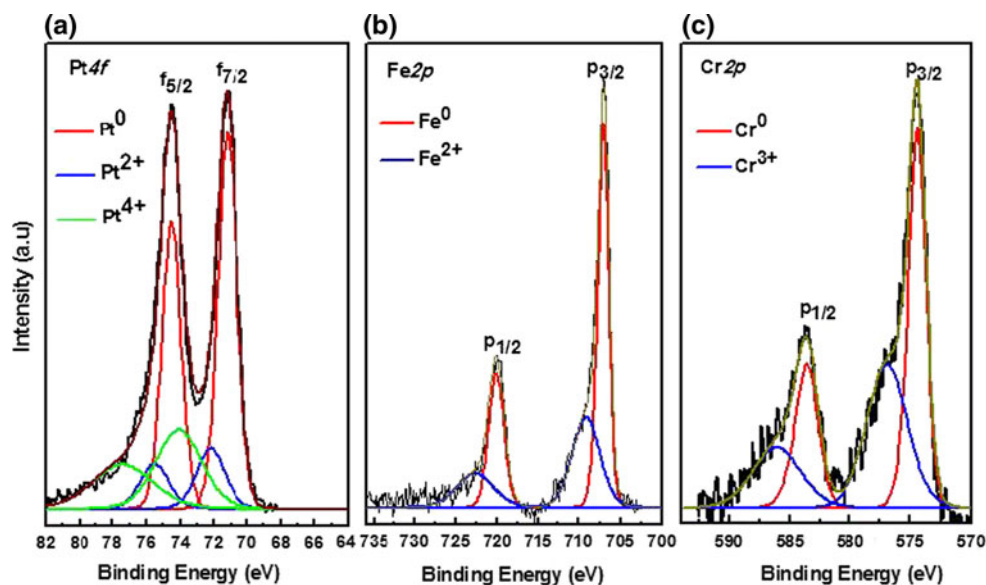
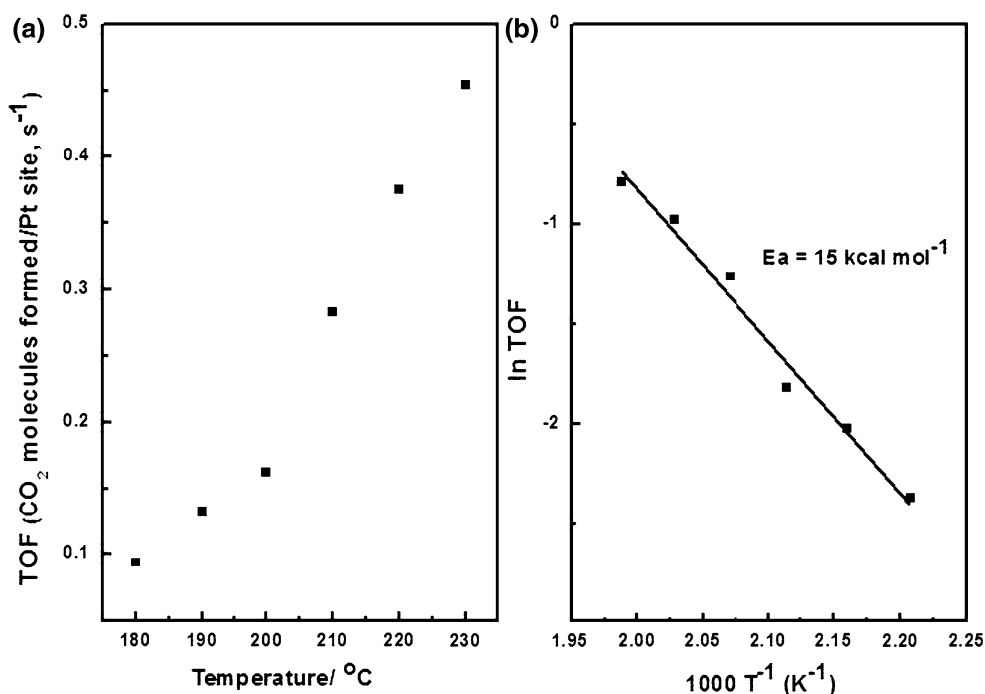


Fig. 5 a CO oxidation activity (turnover rate) of Pt-FeCr alloy nanoparticles as a function of temperature and **b** Arrhenius plots for CO oxidation showing the activation energy of 15 kcal/mol



respectively. The background reaction performed on the FeCr alloy nanoparticles did not show any measurable catalytic activity for CO conversion between 180 and 230 °C. Therefore, the measured catalytic activity on the Pt-FeCr alloy nanoparticles can be exclusively attributed to the Pt nanoparticles. The majority of the crystalline phases of the Pt-FeCr alloy were found to be similar to that of the FeCr alloy with some impurities like Fe_5C_2 and Al_2O_3 [22].

Figure 2 shows the x-ray diffraction patterns of colloidal nanoparticles produced by the electrical explosion of FeCr alloy and Pt wires. XRD peaks corresponding to Pt, Fe and FeCr alloy are present in the sample, indicating the

presence of Pt nanoparticles as a separate phase on the FeCr without any alloy formation with the support. Figure 3 shows a high-resolution transmission electron microscopy (HR TEM) image of Pt-FeCr alloy nanoparticles calcined at 600 °C/30 min. It can be observed that Pt nanoparticles with an average diameter of ~ 2 nm are present on the surface of the FeCr alloy with no particle aggregation. The Pt nanoparticles are spherical with uniform dispersion on the support even after calcination at 600 °C. The EWE method produced highly dispersed Pt nanoparticles on the support, corroborating the XRD findings, akin to conventional synthesis methods for supported

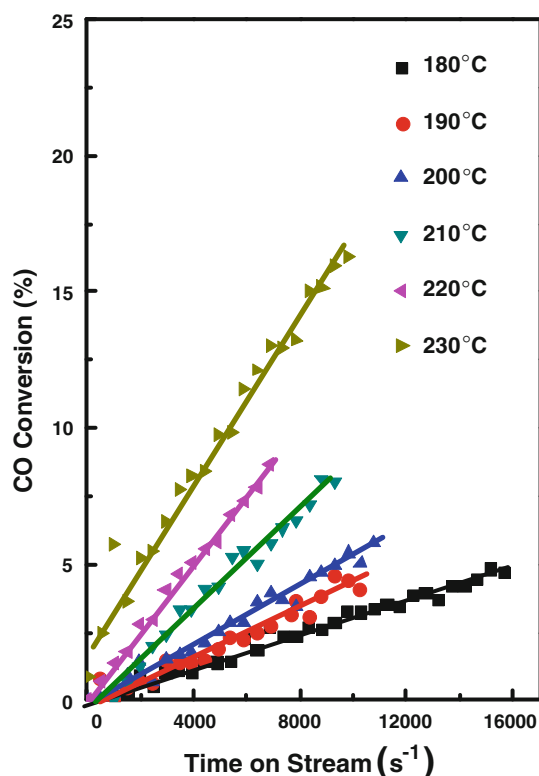


Fig. 6 The catalytic turnover as a function of reaction time at different temperatures measured on Pt-FeCr alloy nanoparticles under CO oxidation

metal catalysts. Pt was deposited on the surface without any indication of alloy formation despite the high operating temperatures ($>10^4$ K) of the EWE process. The uniform dispersion of the Pt metal on the support is mainly due to the sequential explosion of the FeCr and Pt alloy wires, respectively.

Figure 4 shows the x-ray photoelectron spectra of Pt-FeCr alloy nanoparticles after calcination at 600 °C in air/30 min. Surface analysis of the Pt-FeCr alloy nanoparticles shows peaks corresponding to all of the constituent elements [27]. Figure 5a reveals XPS peaks corresponding to Pt4f. A deconvoluted spectrum shows the presence of the main peak ($f_{7/2}$) at 71.2, 72.2 and 74.1 eV, which can be assigned to Pt^0 (58%), Pt^{+2} (13.5%), and Pt^{+4} (28.4%), respectively [27, 28]. Figure 5b shows a photoemission spectrum of the Fe2p main peak ($p_{3/2}$) with a binding energy value of 707.0 and 709.1 eV, indicating the presence of metallic Fe (62%) and Fe^{2+} (38%) [29], respectively. Figure 5c shows a XPS of Cr2p with binding energy values of the main peak ($p_{3/2}$) at 574.4–576.9 eV. These binding energies can be attributed to Cr^0 (52.4%) and Cr^{3+} (47.6%) [27, 28], respectively. Using the sensitivity factors of Pt4f, Fe2p, and Cr2p and the integrated peak areas of each peak, the alloy surface compositions were estimated. The ratio of the surface composition of Fe to that of Cr was

2.8, close to the ratio of the bulk composition of the FeCr alloy (~ 3). Some oxides of Fe and Cr were observed in the XPS data, presumably because of the synthesis in ethanol. Prior to CO oxidation, the catalysts were reduced in H_2/He at 300 °C for 2 h.

CO oxidation was performed on a thin film of Pt-FeCr alloy nanoparticles prepared by the drop casting method and reduced under H_2/He at 300 °C for 1 h. Pt loading on the FeCr alloy nanoparticles were found to be 2.6 wt% (ICP-AES) and Pt dispersion about 46% (calculated from TEM images). Based on these values, the turnover rate was obtained under catalytic CO oxidation. Figure 5a shows the catalytic activity on the Pt-FeCr alloy nanoparticles as a function of temperature at 1 atm. Figure 5b shows the corresponding Arrhenius plots for CO oxidation. From the slope, the activation energy of 15 kcal/mol was calculated. This value is lower than that of Pt single crystals (30–40 kcal/mol) or Pt nanoparticles (25–30 kcal/mol) on various oxide supports [8, 30]. The lowering of the activation energy on this alloy nanocatalyst may be due to a synergic effect between the Pt nanoparticles and the FeCr alloy. The turnover frequency of the Pt-FeCr alloy nanoparticles at 200 °C is 0.16 (/s/Pt site), as can be seen in Fig. 5a. This value is slightly lower than that of Pt nanoparticles (0.2–0.6/s/Pt site) [26] at 200 °C presumably because of the presence of carbonate species formed during the EWE and calcination processes.

This result suggests that the Pt-FeCr alloy nanoparticles can be good catalytic materials for Pt- or Fe-based catalysis, such as diesel oxidation or ammonia synthesis. Figure 6 shows the rate of CO oxidation on the Pt-FeCr alloy nanocatalysts as a function of reaction time at various temperatures. It can be observed that, at a given temperature, CO oxidation increased linearly without any deactivation. The rate of CO oxidation increased linearly as the temperature increased from 180 to 230 °C, showing the absence of deactivation. As alloys are known to increase the melting temperature compared to pure metal particles, FeCr alloys demonstrate outstanding thermal stability compared to other iron-based alloys and they have been used in the fabrication of catalyst supports, gas burners, industrial heaters, and other high-temperature devices [31, 32]. The absence of catalytic deactivation indicates that the interface mixing between the Pt nanoparticles and FeCr alloy can be ignored.

Platinum is a well-known catalyst metal, as well as an expensive and widely studied metal for diesel oxidation in internal combustion engines [33]. It is necessary to explore possible opportunities to reduce the Pt content in catalyst systems for economic reasons, while not compromising catalytic activity. There has been a great deal of research activity to develop Pt-based hybrid nanocatalysts with high catalytic activity and thermal stability, including core-shell

and bimetallic nanocatalysts [8, 30]. The synthesis of Pt-FeCr alloy nanoparticles by the EWE method can provide novel nanocatalysts that have high catalytic activity and good thermal stability.

4 Conclusions

Rapid and large-scale synthesis using the electrical wire explosion process for thermally stable supported Pt nanoparticles for catalytic applications has been demonstrated. By this method, highly dispersed Pt nanoparticles with an average size of 2 nm were produced. This synthesis method is advantageous over conventional methods for ultra small nanoparticles, is versatile, and can be extended for many metals and supports. The high thermal stability of these nanoparticles is useful to investigate mechanisms at higher reaction temperatures and ignition behaviors. CO oxidation on the Pt-FeCr alloy nanoparticles was carried out, and it was found that the Pt-FeCr alloy nanoparticles are active for CO oxidation with an activation energy of 15 kcal/mol and negligible deactivation.

Acknowledgments This work was supported by a grant from the Fundamental R&D Program for Core Technology of Materials funded by the Ministry of Knowledge Economy, Republic of Korea, and by WCU (World Class University) program (31-2008-000-10055-0), and KRF-2011-0015387 through the National Research Foundation of Korea.

References

1. Cui HT, Feng YM, Ren WZ, Zeng T, Lv HY, Pan YF (2009) *Recent Pat Nanotech* 3:32
2. Hiramatsu H, Osterloh FE (2004) *Chem Mater* 16:2509
3. Vesper G, Cao A (2010) *Nat Mater* 9:75
4. Somorjai GA, Park JY (2008) *Angew Chem Int Edit* 47:9212
5. Somorjai GA, Park JY (2008) *Top Catal* 49:126
6. Rioux RM, Song H, Hoefelmeyer JD, Yang P, Somorjai GA (2005) *J Phys Chem B* 109:2192
7. Park JY, Zhang Y, Grass M, Zhang T, Somorjai GA (2008) *Nano Lett* 8:673
8. Joo SH, Park JY, Tsung CK, Yamada Y, Yang PD, Somorjai GA (2009) *Nat Mater* 8:126
9. Westerberg S, Wang C, Chou K, Somorjai GA (2004) *J Phys Chem B* 108:6374
10. Park JY, Lee H, Renzas JR, Zhang YW, Somorjai GA (2008) *Nano Lett* 8:2388
11. Tsirlin T, Zhu J, Grunes J, Somorjai GA (2002) *Top Catal* 19:165
12. Pinna F (1998) *Catal Today* 41:129
13. Zaera F (2003) *Catal Today* 81:149
14. Dumesic JA, Chheda JN, Huber GW (2007) *Angew Chem Int Edit* 46:7164
15. Ciuparu D, Lyubovsky MR, Altman E, Pfefferle LD, Datye A (2002) *Catal Rev* 44:593
16. McCrea KR, Parker JS, Somorjai GA (2002) *J Phys Chem B* 106:10854
17. Pathak A, Pramanik P (2001) *PINSA* 67A:47
18. Karthikeyan J, Berndt CC, Tikkanen J, Wang JY, King AH, Herman H (1997) *Nanostruct Mater* 9:137
19. Gaertner GF, Lydtin H (1994) *Nanostruct Mater* 4:559
20. Katz JL, Miquel PF (1994) *Nanostruct Mater* 4:551
21. Günther B, Kumpmann A (1992) *Nanostruct Mater* 1:27
22. Yun JY, Lee HM, Choi SY, Yang S, Lee DW, Kim YJ, Kim BK (2011) *Mater Trans* 52:250
23. Kinemuchi Y, Murai K, Sangurai C, Cho C-H, Suematsu H, Jiang W, Yatsui K (2003) *J Am Ceram Soc* 86:420
24. Wang Q, Yang H, Shi J, Zou G (2001) *Mater Sci Eng A* 307:190
25. Kwon YS, An VV, Ilyin AP, Tikhonov DV (2007) *Mater Lett* 61:3247
26. Park J, Aliaga C, Renzas J, Lee H, Somorjai G (2009) *Catal Lett* 129:1
27. Aricò AS, Shukla AK, Kim H, Park S, Min M, Antonucci V (2001) *Appl Surface Sci* 172:33
28. Moulder JF, Chastain J, Stickle WF, Sobol PE, Bomben KD (1995) *Handbook of x-ray photoelectron spectroscopy: a reference book of standard spectra for identification and interpretation of XPS data*. Physical Electronics Inc, Eden Prairie
29. Kwon Y-S, Jung Y-H, Yavorovsky NA, Illyn AP, Kim J-S (2001) *Scripta Mater* 44:2247
30. Reddy AS, Kim S, Jeong HY, Jin S, Qadir K, Jung K, Jung CH, Yun JY, Cheon JY, Yang JM, Joo SH, Terasaki O, Park JY (2011) *Chem Commun* 47:8412
31. Lee YY, Kim YH, Chang RW (1994) *J Korean Inst Metals Mater* 32:46
32. Cookson EJ, Floyd DE, Shih AJ (2006) *Int J Mech Sci* 48:1314
33. Kim CH, Qi G, Dahlberg K, Li W (2010) *Science* 327:1624